

# Experimental Advances on Light Baryon Spectroscopy at BESIII Experiment

Shi Wang<sup>1,2</sup> <sup>1,\*</sup> Hao Liu<sup>1,2</sup> <sup>1,†</sup> Shuangshi Fang<sup>4,5,6</sup> <sup>1,‡</sup> and Xiongfei Wang<sup>1,2,3</sup> <sup>1,§</sup>

<sup>1</sup>*School of Physical Science and Technology, Lanzhou University, Lanzhou 730000, China*

<sup>2</sup>*Lanzhou Center for Theoretical Physics, Key Laboratory of Theoretical Physics of Gansu Province, Key Laboratory of Quantum Theory and Applications of MoE,*

*Gansu Provincial Research Center for Basic Disciplines of Quantum Physics, Lanzhou University, Lanzhou 730000, China*

<sup>3</sup>*Frontiers Science Center for Rare Isotopes, Lanzhou University, Lanzhou 730000, China*

<sup>4</sup>*Institute of High Energy Physics, Beijing 100049, People's Republic of China*

<sup>5</sup>*University of Chinese Academy of Sciences, Beijing 100049, China*

<sup>6</sup>*Institute of Physics, Henan Academy of Sciences, Zhengzhou 450046, China*

(Dated: March 5, 2026)

The BESIII experiment is currently the world's only electron-positron collider operating in the tau-charm physical energy region. Since starting data taking in 2009, BESIII has accumulated the world's largest data set in the center-of-mass energy range of 1.84–4.95 GeV, including approximately 10 billion  $J/\psi$  events and 3 billion  $\psi(3686)$  events, together with extensive data on open-charm hadron pair production near threshold regions. These unique datasets, characterized by high statistics and low background, provide unprecedented experimental conditions for studying light baryon spectroscopy. This article systematically reviews the progress made by BESIII in baryon spectroscopy, with a focus on recent breakthrough achievements, including the discovery of excited nucleon states,  $\Lambda$  hyperon states,  $\Sigma$  hyperon states,  $\Xi$  hyperon states and  $\Omega^-$  hyperon states. These results expand the spectrum of baryon excited states and provide crucial experimental support for understanding non-perturbative QCD and resolving the “missing baryon resonances” problem.

## I. INTRODUCTION

Baryons are hadrons composed of three quarks, and their spectral structure serves as an ideal probe for testing non-perturbative effects in Quantum Chromodynamics (QCD). According to the quark model [1–7], baryons should exhibit a rich spectrum of excited states, analogous to the energy level structure in atoms. However, the number of excited states predicted by theory far exceeds the number observed experimentally, making the “missing baryon resonances” problem one of the central puzzles in baryon physics [8, 9]. This discrepancy between theory and experiment suggests that our understanding of non-perturbative QCD remains incomplete, potentially involving complex dynamics not fully captured by the quark model, such as pentaquark components, exotic state contributions, or multi-quark correlation effects.

The BESIII detector at the BEPCII collider, with its low-background environment, high statistics, and broad energy coverage at center-of-mass (c.m.) energy ( $\sqrt{s}$ ) range of 1.84–4.95 GeV, provides a unique experimental platform for baryon spectroscopy [10]. The advantages of the BESIII experiment are threefold: First, operating as a tau-charm factory, it can collect a large number of charmonium decay events, serving as a clean source for the production of baryon excited states. Second, it can take data near the production thresholds of open-charm hadron pairs, effectively suppressing the background and enabling the full reconstruction of

charmed baryons. Third, the detector has excellent charged and neutral particle identification capabilities, combined with advanced reconstruction algorithms, ensuring precise measurements of complex final states. As the only currently operating tau-charm factory, the BESIII experiment not only enables systematic studies of light-flavor baryons including strange baryons, but also provides clean data samples near the production thresholds of charmed baryon pairs, opening new avenues for charmed baryon research. Since data collection began in 2009, the BESIII experiment has achieved a series of breakthroughs in baryon spectroscopy, profoundly advancing our understanding of hadron structure and strong interaction dynamics.

In this article, we provide a concise overview of current experimental progress in light baryon spectroscopy with a focus on results from BESIII experiment, which includes the excited states of nucleon,  $\Lambda$ ,  $\Sigma$ ,  $\Xi$  and  $\Omega$ . Notably, as BESIII continues to accumulate high-precision data, it has emerged as a leading facility for probing hadron structure and testing non-perturbative nature of strong interaction in light baryon spectroscopy. We therefore highlight its recent advances in this field.

## II. BESIII EXPERIMENT

Over the past decades, the understanding of excited-state hyperons composed of three light quarks has primarily relied on the analysis of  $\bar{K}N$  scattering. Due to the use of outdated detectors with poor resolution, some resonances listed by the PDG [11] have not been further investigated for many years. In recent years, with the operation of the BESIII experiment, the charmonium decays produced in  $e^+e^-$  annihilation pro-

\* wangshi@ihep.ac.cn

† lhao2023@lzu.edu.cn

‡ fangss@ihep.ac.cn

§ wangxiongfei@lzu.edu.cn

cesses provide unique opportunities for studying baryon resonances. Their low signal-to-noise ratio and background levels, combined with high energy resolution and large data samples, create favorable conditions for in-depth exploration of potential decay channels.

As schematically illustrated in Fig. 1, the BESIII detector [12] is designed to record symmetric  $e^+e^-$  collisions produced by the BEPCII storage ring [13]. Operating at  $\tau$ -charm physical energy region, i.e.  $\sqrt{s} = 1.84$  and 4.95 GeV. BESIII so far has acquired large data samples across this energy range [10, 14, 15]. The cylindrical core of the BESIII detector encompasses 93% of the full solid angle and comprises a helium-based multilayer drift chamber, a time-of-flight system, and a CsI(Tl) electromagnetic calorimeter. These components are enclosed within a superconducting solenoid magnet that delivers a 1.0 T magnetic field (0.9 T during 2012). An octagonal flux-return yoke, instrumented with resistive plate counters for muon identification interleaved with steel plates, supports the magnet system. The detector provides a charged-particle and photon acceptances of 93% over the full  $4\pi$  solid angle. The momentum resolution for charged particles is 0.5% at 1 GeV/ $c$ , and the  $dE/dx$  resolution for electrons from Bhabha scattering is 6%. In the electromagnetic calorimeter, the energy resolution for photons is 2.5% in the barrel and 5% in the end cap regions at 1 GeV. The time resolution of the plastic scintillator TOF system is 68 ps in the barrel and 110 ps in the end caps. The TOF end cap system was upgraded in 2015 using multi-gap resistive plate chamber technology, providing a time resolution of 60 ps, which benefits the data quality [16–18].

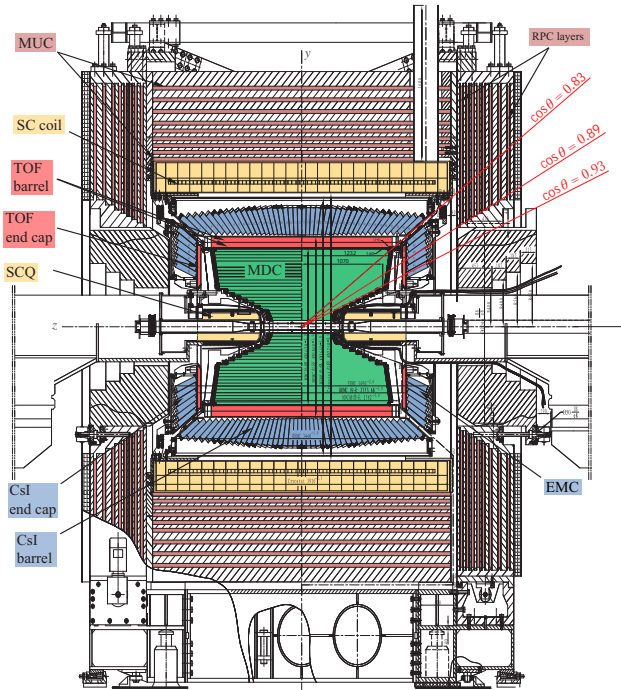


FIG. 1. Schematic diagram of the BESIII detector.

### III. METHODOLOGY

In investigations of excited baryons, one significant challenge arises from their broad widths due to short lifetimes, while another major difficulty is the substantial overlap among different excited states resulting from closely spaced masses. The partial wave analysis (PWA) technique can help address these challenges by disentangling various resonances and determining their properties, including mass, width, spin-parity quantum numbers  $J^P$ , and partial decay widths. Compared with traditional approaches, the PWA method fully utilizes the four-momentum information of final-state particles. In the PWA, the four-momentum-related amplitude construction will be separated into the angle-dependent part and the energy-dependent part. The angular part can be represented as a rotation matrix in the helicity formalism or included in the tensor form amplitude in the covariant tensor formalism so that the information of  $J^P$  of each resonance can be extracted. The energy part is often parameterized using the Breit-Wigner propagator with Blatt-Weisskopf barrier factor [19]. The total amplitude is then fitted to experimental data to determine parameters such as the magnitude and phase of each partial wave, as well as the mass and width of each resonance. Thus, a cascade amplitude expansion can be applied to any decay process to analyze possible resonances in detail. To construct the full decay amplitude, the helicity formalism is used in conjunction with the isobar model, where the three-body decay is described as a two-step sequential quasi-two-body decay. For each two-body decay  $0 \rightarrow 1 + 2$ , the helicity amplitude can be written as

$$A_{\lambda_0, \lambda_1, \lambda_2}^{0 \rightarrow 1+2} = H_{\lambda_1, \lambda_2}^{0 \rightarrow 1+2} D_{\lambda_0, \lambda_1 - \lambda_2}^{J_0^*}(\phi, \theta, 0), \quad (1)$$

where the amplitude  $H_{\lambda_1, \lambda_2}^{0 \rightarrow 1+2}$  is given by the  $LS$  coupling formula [20] along with the barrier factor terms

$$H_{\lambda_1, \lambda_2}^{0 \rightarrow 1+2} = \sum_{l_s} g_{l_s} \sqrt{\frac{2l+1}{2J_0+1}} C_{0, \delta}^{J_0} C_{\lambda_1, -\lambda_2}^s q^l B_l'(q, q_0, d), \quad (2)$$

where  $q$  denotes the breakup momentum in the rest frame of particle 0,  $l$  is the orbital angular momentum,  $g_{l_s}$  are the fit parameters,  $J_{0,1,2}$  are the spins of particles 0, 1, and 2,  $\lambda_{1,2}$  are the helicities for particles 1 and 2, and  $\delta = \lambda_1 - \lambda_2$  is the helicity difference. The  $C_{0, \delta}^{J_0} = \langle l0; s\delta | J_0 \delta \rangle$  and  $C_{\lambda_1, -\lambda_2}^s = \langle J_1 \lambda_1; J_2 (-\lambda_2) | s\delta \rangle$  are Clebsch-Gordan Coefficients. The factor  $B_l'(q, q_0, d)$  is the reduced Blatt-Weisskopf barrier factor [19]. The amplitude for a complete decay chain is constructed as the product of each two body decay amplitude and the resonant propagator  $R$ . For example, in the sequential decays  $0 \rightarrow R_{12} + 3$ ,  $R_{12} \rightarrow 1 + 2$ , the amplitude is written as

$$A_{\lambda_0, \lambda_1, \lambda_2, \lambda_3}^{0 \rightarrow R_{12}+3, R_{12} \rightarrow 1+2} = \sum_{\lambda_{R_{12}}} A_{\lambda_0, \lambda_{R_{12}}, \lambda_3}^{0 \rightarrow R_{12}+3} R(m) A_{\lambda_{R_{12}}, \lambda_1, \lambda_2}^{R_{12} \rightarrow 1+2}. \quad (3)$$

## IV. ADVANCES ON LIGHT BARYON SPECTROSCOPY

To gain a deeper understanding of hadron structure and the dynamics of strong interactions, high-precision experimental studies in light baryon spectroscopy are essential. Recent progress, largely driven by the BESIII experiment and other related facilities, has led to significant achievements in this area. These findings provide groundbreaking insights into hadron structure and strong interactions, while also advancing our comprehension of non-perturbative QCD. In the following sections, we will discuss these experimental advances in detail, with charge-conjugate modes implied throughout unless otherwise stated.

### A. Nucleon excited states

In traditional studies of nucleon excited states, using tagged photons or pion beams [21–24], both the isospin 1/2 and isospin 3/2 resonances are excited, further complicating the analysis. An alternative method for studying nucleon resonances involves the decays of charmonium states such as  $J/\psi$  and  $\psi(3686)$  produced in  $e^+e^-$  collider. By focusing on specific decay channels, such as  $\psi(3686) \rightarrow p\bar{p}\pi^0$ , one can study intermediate  $N^*$  resonances that couple to  $p\pi^0$  or  $\bar{p}\pi^0$ . In such processes,  $\Delta$  resonances are suppressed due to isospin constraints. Moreover,  $\Delta$  states typically exhibit significantly broader widths in the mass spectrum, making their separation from background or non-resonant contributions challenging. As a result,  $\Delta$  resonances are generally excluded from standard analyses, and the reduced number of states substantially simplifies the procedure [25].

The nucleon excited states  $N(2300)$  and  $N(2570)$ , initially observed by BESIII in the decay  $\psi(3686) \rightarrow p\bar{p}\pi^0$  [26], have been confirmed in the decay  $\psi(3686) \rightarrow \bar{p}K^+\Sigma^0$  [27]. Their  $J^P$  assignments, masses, and widths are all consistent with the PDG [11]. Recently, BESIII reported the observation of  $N^*$  and other excited states via  $\psi(3686) \rightarrow p\bar{p}\pi^0$  and  $p\bar{p}\eta$  using a data sample of 2.7 billion  $\psi(3686)$  events [28]. A PWA was performed in this study, and all resonances were parameterized using the Breit-Wigner function with an energy-dependent width  $\Gamma$  [23]. In this analysis, except for several  $N^*$  resonances, other states with masses above 1.8 GeV were also determined. No additional states beyond those listed in the PDG [11] were observed. Figures 2 and 3 show the Dalitz plots of  $M_{p\pi^0/\eta}^2$  versus  $M_{\bar{p}\pi^0/\eta}^2$ , as well as the invariant mass spectra of  $p\pi^0/\eta$  and  $\bar{p}\pi^0/\eta$ . Table I summarized the results of nucleon excited states from BESIII experiment.

### B. $\Lambda$ excited states

The  $\Lambda$  baryon is an isospin singlet, so the production process is strictly constrained if isospin symmetry is conserved. Benefiting from the large data sample and suit-

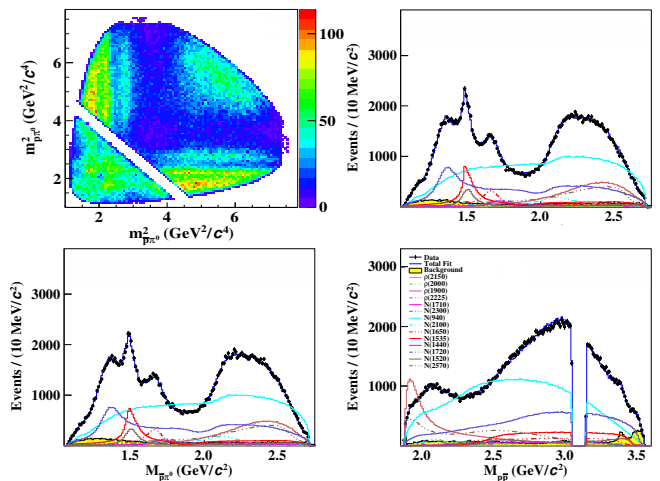


FIG. 2. Dalitz plot of  $M_{p\pi^0}^2$  versus  $M_{\bar{p}\pi^0}^2$  and distributions of  $M_{p\bar{p}}$ ,  $M_{p\pi^0}$  and  $M_{\bar{p}\pi^0}$  in  $\psi(3686) \rightarrow p\bar{p}\pi^0$  from BESIII experiment [28].

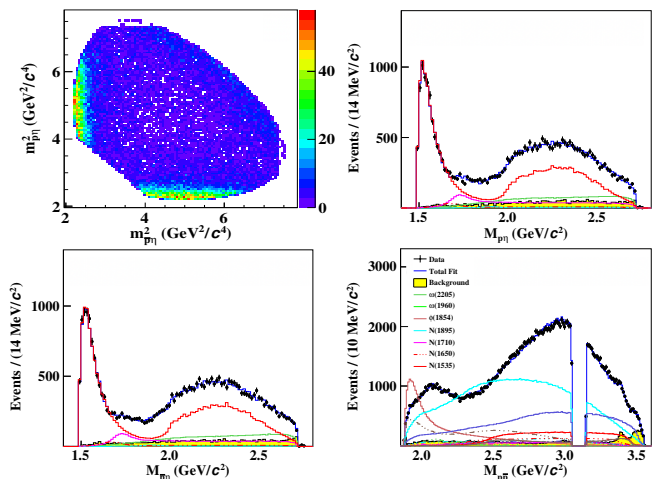


FIG. 3. Dalitz plot of  $M_{p\eta}^2$  versus  $M_{\bar{p}\eta}^2$  and distributions of  $M_{p\bar{p}}$ ,  $M_{p\eta}$  and  $M_{\bar{p}\eta}$  in  $\psi(3686) \rightarrow p\bar{p}\eta$  from BESIII experiment [28].

able phase-space coverage, several resonances have been observed via PWA at BESIII. In 2022, BESIII studied the decay  $\psi(3686) \rightarrow \Lambda\bar{\Lambda}\eta$  and identified the  $\Lambda(1670)$  resonance near the threshold in the  $\eta\Lambda/\bar{\Lambda}$  invariant mass spectrum [29]. The corresponding distributions are shown in Fig. 4. The measured mass and width are  $(1672 \pm 5 \pm 6)$  MeV/ $c^2$  and  $(38 \pm 10 \pm 19)$  MeV, respectively, and the spin-parity  $J^P$  is determined to be  $1/2^-$ , consistent with the PDG values [11]. In the same year, a study of  $\psi(3686) \rightarrow \Lambda\bar{\Lambda}\omega$  [30] reported a new resonance labeled  $\Lambda(2000)$ , as shown in Fig. 5, with a significance of only  $3\sigma$ . Its extracted width is considerably narrower than any known state listed in the PDG [11], suggesting the need for further investigation. In 2023, studies of  $e^+e^- \rightarrow pK^-\bar{\Lambda}$  at 4.178 GeV [31] and  $J/\psi \rightarrow \Sigma^\mp \bar{\Lambda}\pi^\pm$  [32] did not reveal or measure any  $\Lambda^*$  resonances, though the former analysis reported a new  $1^+$  resonance, denoted  $K_1(2085)$ , in the  $p\bar{\Lambda}$  mass spectrum. In 2025, the BE-

TABLE I. Summary of mass, width and branching fraction for the nucleon resonances. The first uncertainties are statistical and the second systematic.

Mode	Resonance	Mass (MeV/ $c^2$ )	Width (MeV)	$\mathcal{B}$ ( $\times 10^{-6}$ )
$\psi(3686) \rightarrow \bar{p}K^+\Sigma^0$ [27]	$N(2300)$	$2285.3 \pm 13.8 \pm 26.1$	$335.9 \pm 14.6 \pm 21.6$	$1.95 \pm 0.53 \pm 0.58$
	$N(2570)$	$2577.9 \pm 14.8 \pm 33.2$	$255.1 \pm 14.6 \pm 19.7$	$2.28 \pm 0.53 \pm 0.67$
$\psi(3686) \rightarrow p\bar{p}\pi^0$ [28]	$N(1440)$	—	—	$54.2 \pm 1.4 \pm 14.1$
	$N(1520)$	—	—	$6.6 \pm 0.4 \pm 2.0$
	$N(1535)$	—	—	$17.5 \pm 0.7 \pm 3.6$
	$N(1650)$	—	—	$9.1 \pm 0.7 \pm 3.2$
	$N(1710)$	—	—	$4.2 \pm 0.5 \pm 4.0$
	$N(1720)$	—	—	$6.2 \pm 0.5 \pm 2.4$
	$N(2100)$	—	—	$8.5 \pm 0.9 \pm 3.8$
	$N(2300)$	—	—	$3.6 \pm 0.6 \pm 3.0$
$\psi(3686) \rightarrow p\bar{p}\eta$ [28]	$N(2570)$	—	—	$19.5 \pm 0.9 \pm 14.5$
	$N(1535)$	—	—	$50.5 \pm 1.3 \pm 7.1$
	$N(1710)$	—	—	$7.8 \pm 0.7 \pm 3.1$

SIII collaboration reported a significant signal of the  $\Lambda(2325)$  state in the decay  $\psi(3686) \rightarrow \Lambda\bar{\Sigma}^0\pi^0$  [33]. The corresponding mass spectrum fit curves are shown in Fig. 6. Additionally, the two-pole structure of  $\Lambda(1405)$  was investigated using two independent parameterizations: a Flatté-like model [34] and a chiral dynamics approach [35]. However, due to limited statistics, it was not possible to determine which model provides a better description of the data. Therefore, both parameterization results are reported in this analysis.

Recently, the BESIII collaboration has reported observations of  $\Lambda(1690)$  and  $\Lambda(1810)$  in the isospin-violating process  $J/\psi \rightarrow \Lambda\bar{\Sigma}^0\eta$ , as illustrated in the Dalitz plots in Fig. 7. The measured mass of  $\Lambda(1810)$  is approximately 90 MeV/ $c^2$  higher than the PDG-accepted value of 1790 MeV/ $c^2$  [11], though the results remain consistent within two standard deviations. This measured mass is also consistent with predictions from quark model calculations [36]. Given the proximity of its mass to that of  $\Lambda(1890)$  with  $J^P = 3/2^+$ , an alternative fit was performed by replacing  $\Lambda(1810)$  with  $\Lambda(1890)$ , which led to a slightly worse fit quality. Based on the currently limited statistics, we conclude that the presence of  $\Lambda(1890)$  cannot be ruled out. Table II summarized the recent results of  $\Lambda$  excited states from BESIII experiment.

### C. $\Sigma$ excited states

Recent advances in our understanding of  $\Sigma$  excited states have been driven largely by multi-channel analyses of  $\bar{K}N$  scattering data [38, 39]. Nevertheless, several predicted  $\Sigma$  resonances remain unobserved compared to theoretical expectations [40]. With the world's largest data samples of  $J/\psi$  and  $\psi(3686)$  events, the BESIII experiment offers a unique opportunity to systematically investigate these missing  $\Sigma$  states.

In the study of  $\Sigma$  baryons, the BESIII collaboration analyzed the decay  $\psi(3686) \rightarrow \bar{p}K^+\Sigma^0$  [27], and identified a new excited  $\Sigma$  state,  $\Sigma(2330)$ , with a statistical significance of

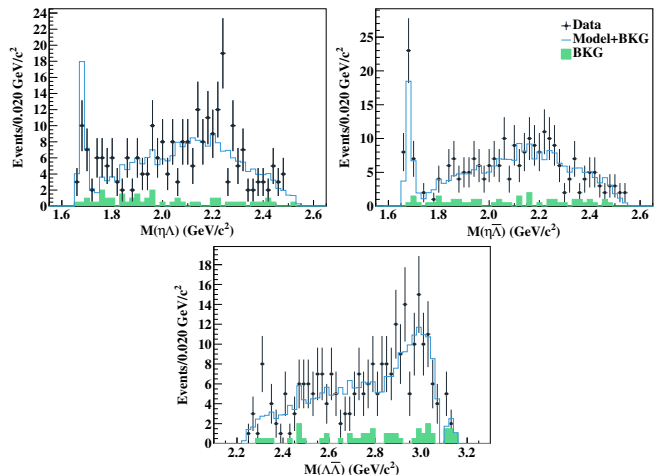


FIG. 4. Distributions of  $M(\eta\Lambda)$ ,  $M(\eta\bar{\Lambda})$  and  $M(\Lambda\bar{\Lambda})$  in  $\psi(3686) \rightarrow \Lambda\bar{\Lambda}\eta$  from BESIII experiment [29].

$11.9\sigma$  in the  $M_{\bar{p}K^+}$  distribution, as illustrated in Fig. 8. The measured mass and width are  $(2334.7 \pm 7.9 \pm 16.0)$  MeV/ $c^2$  and  $(206.3 \pm 9.5 \pm 18.4)$  MeV, respectively, where the first uncertainty is statistical and the second systematic. The spin-parity assignment for  $\Sigma(2330)$  favors  $3/2^-$ . No known resonance in the PDG [11] corresponds to both its mass and width. A recent theoretical prediction [40] attributes excited  $\Sigma$  states near 2.33 GeV/ $c^2$  to the 1F family. Our result is consistent with the predicted 1F( $3/2^-$ ) state within 5 MeV/ $c^2$ . Alternative spin-parity assignments of  $3/2^+$  and  $5/2^-$  yield significances of  $10.7\sigma$  and  $11.0\sigma$ , respectively—values very close to that of the nominal  $3/2^-$  hypothesis. Due to limited statistics and the proximity of the  $\Sigma(2330)$  mass to the phase-space threshold, the current data cannot definitively discriminate among these possibilities. Further studies with larger datasets and additional decay channels will be necessary to unambiguously determine the quantum numbers of  $\Sigma(2330)$ . Furthermore, spin-parity analyses were carried out for the one-star

TABLE II. Summary of mass, width and branching fraction for the  $\Lambda$  resonances. The first uncertainties are statistical and the second systematic.

Mode	Resonance	Mass ( $\text{MeV}/c^2$ )	Width (MeV)	$\mathcal{B} (\times 10^{-5})$
$\psi(3686) \rightarrow \Lambda \bar{\Lambda} \eta$ [29]	$\Lambda(1670)$	$1672 \pm 5 \pm 6$	$38 \pm 10 \pm 19$	$1.29 \pm 0.31 \pm 0.62$
$\psi(3686) \rightarrow \Lambda \bar{\Lambda} \omega$ [30]	$\Lambda^*$	$2001 \pm 7$	$36 \pm 14$	$< 1.40$ (@ 90% CL)
$\psi(3686) \rightarrow \Lambda \bar{\Sigma}^0 \pi^0$ [33]	$\Lambda(1405)$	—	—	$0.44 \pm 0.05 \pm 0.12$
	$\Lambda(1520)$	$1519.9 \pm 1.6 \pm 4.8$	$20.6 \pm 1.9 \pm 0.6$	$0.19 \pm 0.05 \pm 0.05$
	$\Lambda(1600)$	$1570.5 \pm 4.6 \pm 12.1$	$228.1 \pm 11.9 \pm 34.8$	$4.49 \pm 0.25 \pm 1.23$
	$\Lambda(1670)$	$1667.5 \pm 2.3 \pm 3.6$	$30.2 \pm 1.2 \pm 1.8$	$0.33 \pm 0.07 \pm 0.09$
	$\Lambda(1690)$	$1691.1 \pm 4.4 \pm 15.7$	$72.3 \pm 4.7 \pm 18.3$	$0.55 \pm 0.11 \pm 0.10$
	$\Lambda(1800)$	$1800.9 \pm 2.3 \pm 4.2$	$13.3 \pm 2.5 \pm 4.5$	$12.6 \pm 2.5 \pm 4.5$
	$\Lambda(1890)$	$1897.2 \pm 2.3 \pm 4.2$	$9.6 \pm 2.5 \pm 4.5$	$6.2 \pm 2.5 \pm 4.5$
$\psi(3686) \rightarrow \Lambda \bar{\Sigma}^0 \eta$ [37]	$\Lambda(1670)$	$1668.8 \pm 1.2 \pm 1.5$	$3.1 \pm 0.2 \pm 0.3$	$21.2 \pm 0.8 \pm 1.4$
	$\Lambda(1810)$	$1881.5 \pm 2.3 \pm 4.2$	$16.5 \pm 0.7 \pm 0.9$	$20.3 \pm 0.7 \pm 1.4$
$\psi(3686) \rightarrow \bar{p} K^+ \Sigma^0$ [27]	$\Lambda(1520)$	—	—	$0.49 \pm 0.05 \pm 0.14$

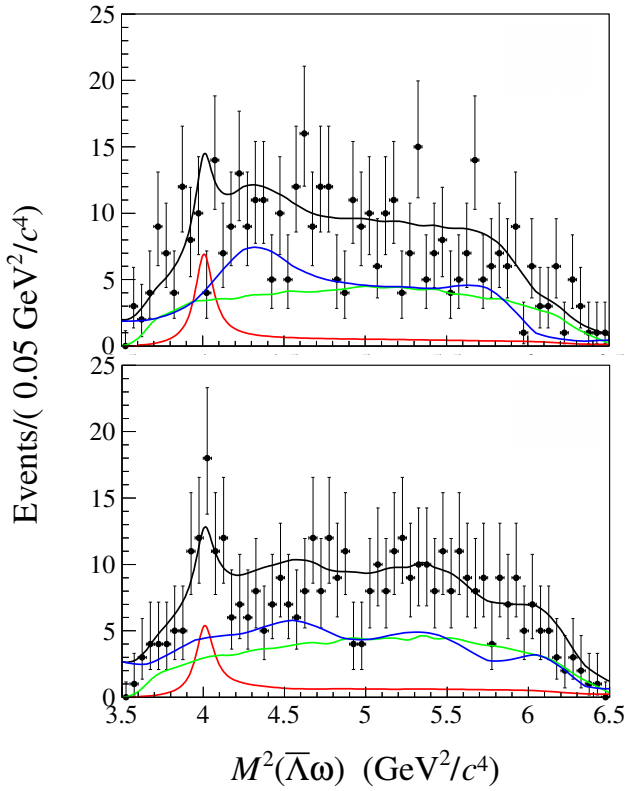


FIG. 5. Distributions of  $M^2(\Lambda\omega)$  (Top) and  $M^2(\bar{\Lambda}\omega)$  (Bottom) in  $\psi(3686) \rightarrow \Lambda \bar{\Lambda} \omega$  from BESIII experiment [30], the red solid curves show the shape of  $\Lambda^*-\bar{\Lambda}^*$  resonances, the blue solid curves show the background described by  $\omega$  sidebands and the green solid curves show the shapes from the non-resonant decay.

states  $\Sigma(2010)$  and  $\Sigma(2110)$ . The results support  $J^P = 3/2^-$  and  $J^P = 1/2^-$ , respectively, in agreement with the assignments given by the PDG [11].

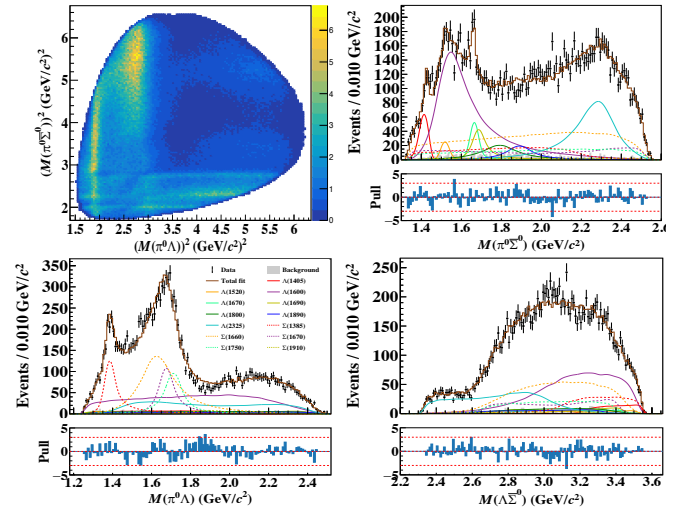


FIG. 6. Dalitz plot of  $M^2(\pi^0 \Lambda)$  versus  $M^2(\pi^0 \bar{\Sigma}^0)$  and distributions of  $M(\Lambda \bar{\Sigma}^0)$ ,  $M(\pi^0 \Lambda)$  and  $M(\pi^0 \bar{\Sigma}^0)$  in  $\psi(3686) \rightarrow \Lambda \bar{\Sigma}^0 \pi^0$  from BESIII experiment [33].

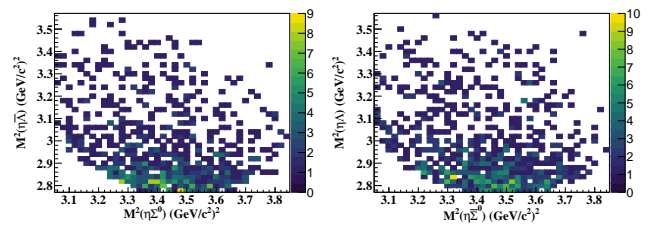


FIG. 7. Dalitz plots of  $M^2(\Lambda \bar{\Sigma}^0)$  versus  $M^2(\eta \bar{\Sigma}^0)$  in  $\psi(3686) \rightarrow \Lambda \bar{\Sigma}^0 \eta$  from BESIII experiment [37].

In the analyses of  $J/\psi \rightarrow \Sigma^\mp \bar{\Lambda} \pi^\pm$  [32] and  $\psi(3686) \rightarrow \Lambda \bar{\Sigma}^0 \pi^0$  [33], several resonances  $\Sigma^*$  are considered in the nominal fit according to the PDG [11], but no new states have been

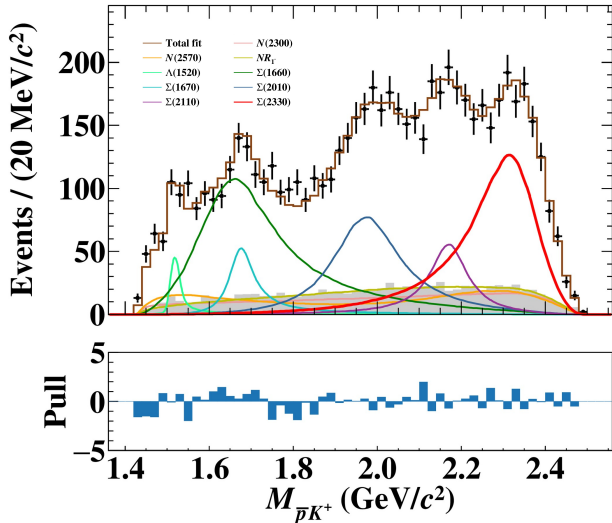


FIG. 8. Distribution of  $M_{\bar{p}K^+}$  from BESIII experiment [27].

confirmed. While in the analysis  $\psi(3686) \rightarrow \Sigma^0 \bar{\Sigma}^0 \omega$  [41], a hint of a resonance in the  $\Sigma^0(\bar{\Sigma}^0)\omega$  invariant mass spectrum is observed, as shown in Fig. 9. The fit to the invariant mass distribution yields a significance of  $2.5\sigma$ , with a measured mass and width of  $(2058 \pm 15)$  MeV/ $c^2$  and  $(65 \pm 18)$  MeV, respectively. However, due to the limited statistics, the intermediate state is not analyzed through PWA method, and its quantum numbers cannot be determined.

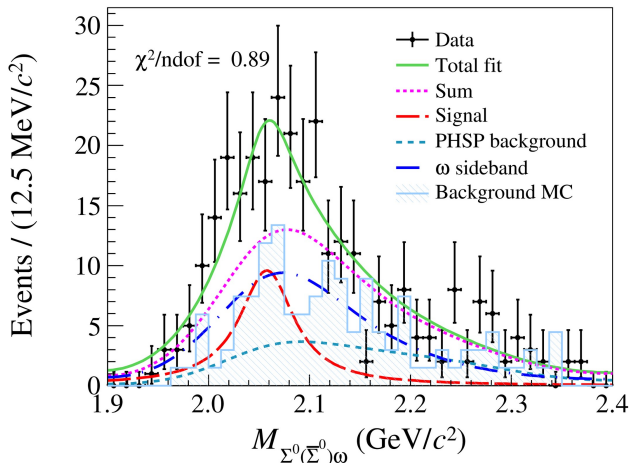


FIG. 9. Distribution of  $M_{\Sigma^0(\bar{\Sigma}^0)\omega}$  from BESIII experiment [41].

In 2025, the BESIII collaboration reported the first evidence for a potential pentaquark state, the  $\Sigma(1380)^+$ , identified in the  $\Lambda\pi^+$  system from the decay  $\Lambda_c^+ \rightarrow \Lambda\pi^+\eta$  [42] using a PWA. In this analysis, the Breit-Wigner mass and width of the  $\Sigma(1380)^+$  were fixed at 1380 MeV/ $c^2$  and 120 MeV, respectively, following predictions from Refs. [43, 44]. To conservatively evaluate the statistical significance of the  $\Sigma(1380)^+$  signal, two models were compared: “model A,” which includes the resonances  $\Lambda a_0(980)^+$ ,  $\Sigma(1385)^+\eta$ ,  $\Lambda(1670)\pi^+$ ,

and  $\Sigma(1380)^+\eta$ ; and “model B,” which adds a non-resonant component with  $J^P = 0^+$  ( $\Lambda\text{NR}_{0^+}$ ) to the resonance set of model A. The corresponding fit curves are presented in Fig. 10. Based on the likelihood differences between fits with and without the  $\Sigma(1380)^+$  resonance, the statistical significances were found to be  $6.1\sigma$  for model A and  $3.3\sigma$  for model B. Table III summarized the recent results of  $\Lambda$  excited states

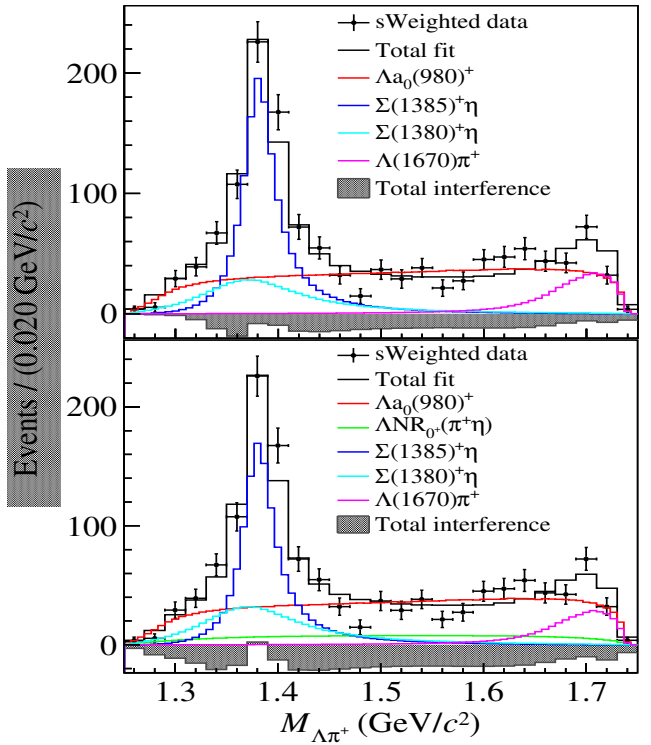


FIG. 10. Distribution of  $M_{\Lambda\pi^+}$  with PWA fits using model A (Top) and model B (Bottom) from BESIII experiment [42].

from BESIII experiment.

#### D. $\Xi$ excited states

The  $\Xi$  baryon is a doubly strange hyperon composed of two strange quarks and one light quark. Compared to singly strange hyperons ( $\Lambda$ ,  $\Sigma$ ),  $\Xi$  baryons have smaller production cross-sections, making their experimental investigation more challenging. For the excited states of the  $\Xi$  baryon, experimental evidence remains limited, with the exception of the well-established  $\Xi(1530)$ . Resonances in the mass region of 1.5 and 1.61 GeV can be easily identified via the  $\Xi\pi$  decay channel, while those with masses above 1.61 GeV may appear in decay channels such as  $\Lambda K$  and  $\Sigma K$ . Taking  $\Xi(1620)$  as an example, this particle was first discovered in the 1970s [45–47]. Recently, the Belle collaboration updated its parameters by analyzing the  $\Xi_c \rightarrow \Xi\pi\pi$  decay process [48], measuring a mass and width of  $(1610.4 \pm 6.0^{+6.1}_{-4.2})$  MeV/ $c^2$  and  $(59.9 \pm 4.8^{+2.8}_{-7.1})$  MeV, respectively. Figure 11 shows the in-

TABLE III. Masses, widths, and production branching fractions of the  $\Xi$  resonances. The first uncertainties are statistical and the second systematic.

Mode	Resonance	Mass (MeV/ $c^2$ )	Width (MeV)	$\mathcal{B} (\times 10^{-5})$
$\psi(3686) \rightarrow \bar{p}K^+\Sigma^0$ [27]	$\Sigma(1660)$	$1680.5 \pm 13.8 \pm 21.3$	$247.7 \pm 15.8 \pm 18.8$	$5.84 \pm 0.69 \pm 1.55$
	$\Sigma(1670)$	$1680.5 \pm 4.1 \pm 11.0$	$73.4 \pm 9.1 \pm 7.1$	$1.22 \pm 0.38 \pm 0.28$
	$\Sigma(2010)$	$1980.1 \pm 10.0 \pm 18.1$	$192.5 \pm 13.3 \pm 13.3$	$3.11 \pm 0.50 \pm 0.92$
	$\Sigma(2110)$	$2172.4 \pm 6.3 \pm 10.9$	$107.2 \pm 9.3 \pm 10.2$	$1.17 \pm 0.23 \pm 0.38$
	$\Sigma(2330)$	$2334.7 \pm 7.9 \pm 16.0$	$206.3 \pm 9.5 \pm 18.4$	$4.47 \pm 0.58 \pm 1.52$
$\psi(3686) \rightarrow \Lambda\bar{\Sigma}^0\pi^0$ [33]	$\Sigma(1385)$	$1388.2 \pm 1.9 \pm 3.3$	$60.5 \pm 3.6 \pm 6.3$	$1.30 \pm 0.11 \pm 0.19$
	$\Sigma(1660)$	$1643.2 \pm 4.5 \pm 7.6$	$221.3 \pm 13.1 \pm 41.1$	$3.53 \pm 0.29 \pm 0.63$
	$\Sigma(1670)$	$1679.7 \pm 3.4 \pm 4.3$	$87.0 \pm 6.4 \pm 8.9$	$1.60 \pm 0.25 \pm 0.38$
	$\Sigma(1750)$	$1714.9 \pm 4.2 \pm 7.3$	$97.2 \pm 9.8 \pm 9.7$	$1.39 \pm 0.23 \pm 0.32$
	$\Sigma(1910)$	$1912.1 \pm 10.6 \pm 33.6$	$225.1 \pm 24.5 \pm 46.0$	$0.23 \pm 0.10 \pm 0.06$
$\psi(3686) \rightarrow \Sigma^0\bar{\Sigma}^0\omega$ [41]	$\Sigma^*$	$2058 \pm 15$	$36 \pm 14$	—

variant mass of  $\Xi^-\pi^+$ . A clear  $\Xi(1620)$  signal can be observed around 1.6 GeV with a significance greater than  $25\sigma$ , while only an evidence of the  $\Xi(1690)$  is found to be a significance of  $4\sigma$ . However, these results exhibit some discrepancies with earlier experiments and have not yet been independently verified by other experiments. Currently, the BESIII collaboration is conducting further tests on the existence of  $\Xi(1620)$  using the process  $e^+e^- \rightarrow \Xi^*\bar{\Xi}$ .

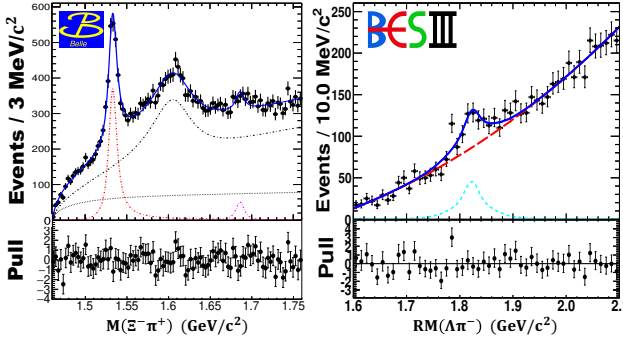


FIG. 11. Distributions of  $M(\Xi^-\pi^+)$  from Belle experiment [48] and  $RM(\Lambda\pi^+)$  from BESIII experiment [49].

For higher-mass  $\Xi$  excited states, the BESIII collaboration confirmed the existence of  $\Xi(1820)$  in 2020 through the recoil invariant mass spectrum of  $\Xi$  baryons while measuring the  $e^+e^- \rightarrow \Xi^-\bar{\Xi}^+$  cross section at  $\sqrt{s} = 4.0$ - $4.6$  GeV energy region [49]. A Breit-Wigner fit yielded a mass and width of  $(1825.5 \pm 4.7 \pm 4.7)$  MeV/ $c^2$  and  $(17.0 \pm 15.0 \pm 7.9)$  MeV, respectively. This marks the first update of the particle's parameters since the WA89 experiment [50], with significantly improved measurement precision, though its spin-parity quantum numbers remain undetermined. As of 2024, both excited states,  $\Xi(1690)$  and  $\Xi(1820)$ , have been experimentally confirmed. In 2024, the  $\Xi(1690)$  and  $\Xi(1820)$  states were analyzed in the decay process  $\psi(3686) \rightarrow \Lambda K^-\bar{\Xi}^+$  using a PWA approach [51]. The  $\Xi(1690)$  and  $\Xi(1820)$  were ob-

served with the significance of greater than  $10\sigma$  as shown in Fig. 12. Their masses and widths were determined as  $(1685_{-2}^{+3} \pm 12)$  MeV/ $c^2$  and  $(81_{-9}^{+10} \pm 20)$  MeV for  $\Xi(1690)$ , and  $(1821_{-3}^{+2} \pm 3)$  MeV/ $c^2$  and  $(73_{-5}^{+6} \pm 9)$  MeV for  $\Xi(1820)$ , respectively. The analysis also confirmed the quantum numbers  $1/2^-$  for  $\Xi(1690)$  and  $3/2^-$  for  $\Xi(1820)$ , in agreement with previous results cited by the PDG. Notably, the measured width of  $\Xi(1820)$  is significantly larger than that reported in earlier work, which has prompted theoretical interest [52] regarding the internal structure of this resonance. Figure 13 shows the comparison of resonance parameters for  $\Xi$  excited baryon states.

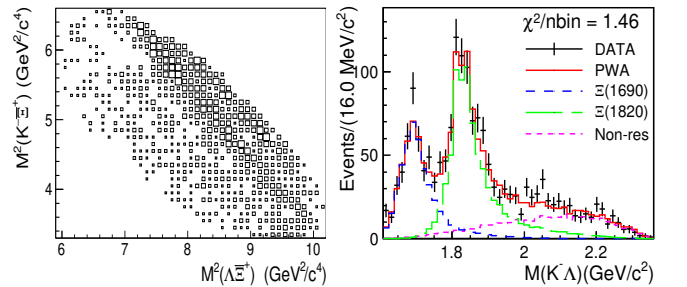


FIG. 12. Dalitz plot of  $M^2(K^-\bar{\Xi}^+)$  versus  $M^2(\Lambda\bar{\Xi}^+)$  and distribution of  $M(K^-\Lambda)$  from BESIII experiment [51].

### E. $\Omega^-$ excited states

The  $\Omega^-$  baryon is a hyperon composed of three strange quarks ( $sss$ ), and the study of its excited states is an important topic in baryon spectroscopy. According to the quark model, the  $\Omega^-$  baryon should possess a rich spectrum of excited states. However, experimental knowledge of these states remains extremely limited. The significant gap between theoretical predictions and experimental observations constitutes one of the core issues of the long-standing ‘‘missing baryon

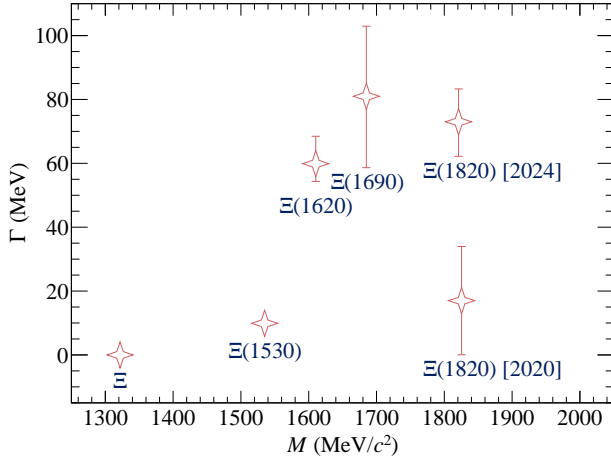


FIG. 13. Comparison of width and mass for  $\Xi$  baryon and its excited states from the Belle and BESIII experiments.

resonances” puzzle that has perplexed the particle physics community for decades. In 2018, the Belle experiment reported the first observation of an excited  $\Omega^-$  baryon, i.e.,  $\Omega(2012)^-$ , in the decay modes of  $\Xi^0 K^-$  and  $\Xi^- K_S^0$  using the data taken in  $\Upsilon(1S)$ ,  $\Upsilon(2S)$ , and  $\Upsilon(3S)$  decays with a significance greater than  $7\sigma$  [53]. The mass and width of  $\Omega(2012)^-$  were measured to be  $(2012.4 \pm 0.7 \pm 0.6) \text{ MeV}/c^2$  and  $\Gamma = (6.4_{-2.0}^{+2.5} \pm 1.6) \text{ MeV}$ . In 2025, Belle also observed the  $\Omega(2012)^-$  baryon with  $\Xi(1530)\bar{K} \rightarrow \Xi\pi\bar{K}$  with a significance of  $5.2\sigma$  [54]. Figure 14 shows the invariant masses of  $\Xi^0 K^-$ ,  $\Xi^- K_S^0$  and  $\Xi^- \pi^+ K^-$ . The mass was measured to be  $(2012.5 \pm 0.7 \pm 0.5) \text{ MeV}/c^2$ , in agreement with the previous result [53]. The effective couplings for  $\Omega(2012)^- \rightarrow \Xi(1530)\bar{K}$  and  $\Xi\bar{K}$  were found to be  $(39 \pm 31 \pm 9) \times 10^{-2}$  and  $(1.7 \pm 0.3 \pm 0.3) \times 10^{-2}$ , respectively. Meanwhile, the Belle measurement on the narrow width implies that the quantum number of  $\Omega(2012)^-$  is more favorable to  $3/2^-$  according to the prediction of theoretical models [36, 55–61].

In recent years, the BESIII experiment has made breakthrough progress in this field. Using a data sample of approximately  $19 \text{ fb}^{-1}$  collected at c.m. energies ranging from 4.13 to 4.70 GeV, the BESIII collaboration developed new research methods and achieved two key discoveries in the study of  $\Omega^-$  baryon excited states. First, in the process  $e^+e^- \rightarrow \Omega(2012)^-\bar{\Omega}^+$ , the research team confirmed the existence of  $\Omega(2012)^-$  with a significance of 3.5 standard deviations [62], validating the resonance state initially reported by the Belle experiment. More importantly, BESIII has, for the first time, found evidence for a new excited state of the  $\Omega^-$  hyperon, with a signal significance of 4.1 standard deviations including systematic uncertainties and the look-elsewhere effect. This new particle has been designated as  $\Omega(2109)^-$ . Figure 14 (Bottom) shows the recoil mass spectrum of  $\Omega^-$ . The experimental measurements yield a mass of  $M = (2108.5 \pm 5.2 \pm 0.9) \text{ MeV}/c^2$  and a width of  $\Gamma = (18.3 \pm 16.4 \pm 5.7) \text{ MeV}$ . These two discoveries hold

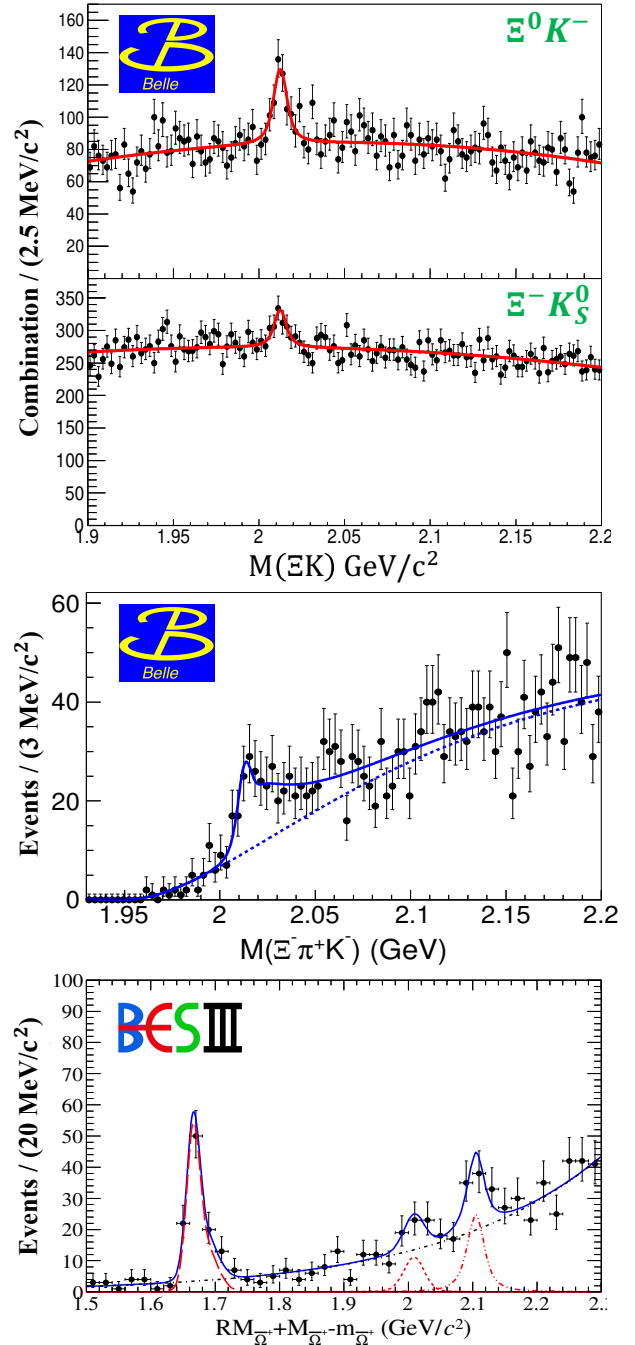


FIG. 14. Distributions of  $M(\Xi^0 K^-)$ ,  $M(\Xi^- K_S^0)$  and  $M(\Xi^- \pi^+ K^-)$  from Belle experiment [53, 54] and  $RM_{\bar{\Omega}^+} + M_{\Omega^-} - m_{\Omega^-}$  from BESIII experiment [62].

significant theoretical implications. The masses of  $\Omega(2012)^-$  and  $\Omega(2109)^-$  are in excellent agreement with predictions from the lattice QCD calculation [63], which had predicted masses of approximately  $2.0 \text{ GeV}/c^2$  and  $2.1 \text{ GeV}/c^2$  for  $\Omega^-$  excited states with spin-parity  $J^P = 1/2^-$  and  $3/2^-$ , respec-

tively. This strong agreement supports the interpretation that  $\Omega(2012)^-$  and  $\Omega(2109)^-$  are likely conventional three-quark states, rather than exotic hadronic molecular states. Meanwhile, the experimentally measured mass of  $\Omega(2109)^-$  exhibits a deviation of approximately 50 MeV below the theoretical predictions [64]. In addition, the theoretical study of Hamiltonian effective field theory suggests that the quantum number of  $\Omega(2012)^-$  could be  $J^P = 3/2^-$  resonance while recently reported  $\Omega(2109)^-$  may be  $J^P = 1/2^-$  [65]. The experimental achievements not only provide crucial experimental evidence for understanding the internal structure of  $\Omega^-$  baryon excited states, but also lay an important foundation for ultimately resolving the “missing baryon resonances” puzzle and refining QCD theory. In the future, with more data accumulation and in-depth analysis, further breakthroughs in  $\Omega^-$  baryon spectroscopy are anticipated. Figure 15 shows the comparison of resonance parameters for  $\Omega^-$  excited baryon states between the experimental measurements and theoretical predictions.

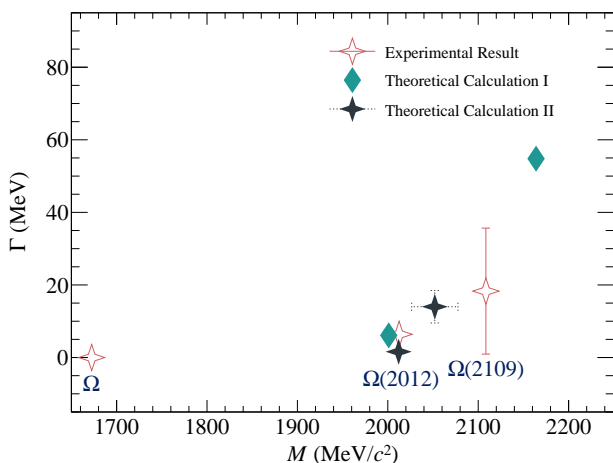


FIG. 15. Comparison of resonance parameters for  $\Omega^-$  baryon and its excited states from the Belle and BESIII experiments, where the theoretical calculations are cited from Ref. [64] and Ref. [65] for the result I and II, respectively.

## V. SUMMARY

Over the past decade of operation, the BESIII experiment has achieved remarkable accomplishments in the field

of baryon spectroscopy. The work of the BESIII collaboration is systematically deepening our understanding of baryon structure. In the study of light-flavored baryon excited states, BESIII has made a series of breakthroughs in the investigation of  $\Sigma$ ,  $\Xi$ , and  $\Omega^-$  hyperon excitations by utilizing 10 billion  $J/\psi$  and 3 billion  $\psi(3686)$  events [10]. These results provide crucial experimental data for addressing the “missing baryon resonances” problem, showing strong consistency with lattice QCD predictions and robustly supporting the quark model’s description of the baryon spectrum. At the same time, they reveal spin-orbit coupling effects that have not been sufficiently considered in the quark model.

Looking ahead, the BESIII experiment continues to accumulate data, with its c.m. energy coverage continuously expanding. According to BESIII’s future physics plan, high-precision measurements will continue in the tau-charm energy region during the remaining operation period, with optimized data acquisition strategies and physics motivations for potential luminosity upgrades. Particularly promising is the Super Tau-Charm Factory in Russia [66] and China [67], which is at the forefront of higher luminosity and has entered the preliminary research stage. Its designed luminosity will be two orders of magnitude higher than that of BEPCII, and it is expected to accumulate a data sample two orders of magnitude larger than that of BESIII. This will advance baryon spectroscopy research to unprecedented precision, making the discovery of more excited states possible. Solving the mystery of the “missing baryon resonances”, refining non-perturbative QCD theory, and testing the precision of the Standard Model. These core objectives of baryon physics are gradually being approached with each new discovery from the BESIII experiment. From  $\Sigma$  hyperon excitations to the  $\Omega^-$  hyperon spectrum, the BESIII experiment is writing a new chapter in the study of baryon spectroscopy.

## VI. ACKNOWLEDGEMENT

This work was supported by the Fundamental Research Funds for the Central Universities Nos. Izujbky-2025-ytA05, Izujbky-2025-it06, Izujbky-2024-jdzx06; the Natural Science Foundation of Gansu Province No. 22JR5RA389, No.25JRRA799; the ‘111 Center’ under Grant No. B20063; the National Natural Science Foundation of China under Contract No. 12225509,12247101.

[1] M. Gell-Mann, A Schematic Model of Baryons and Mesons, *Phys. Lett.* **8**, 214 (1964).  
 [2] S. Capstick and W. Roberts, Quark models of baryon masses and decays, *Prog. Part. Nucl. Phys.* **45**, S241 (2000), [arXiv:nuc-th/0008028](https://arxiv.org/abs/nuc-th/0008028).

[3] L. Y. Glozman, W. Plessas, K. Varga, and R. F. Wagenbrunn, Unified description of light and strange baryon spectra, *Phys. Rev. D* **58**, 094030 (1998), [arXiv:hep-ph/9706507](https://arxiv.org/abs/hep-ph/9706507).  
 [4] L. Y. Glozman and D. O. Riska, The Spectrum of the nucleons and the strange hyperons and chiral dynamics, *Phys. Rept.* **268**, 263 (1996), [arXiv:hep-ph/9505422](https://arxiv.org/abs/hep-ph/9505422).

- [5] C. Menapara and A. K. Rai, Spectroscopic investigation of light strange  $S = -1$   $\Lambda$ ,  $\Sigma$  and  $S = -2$   $\Xi$  baryons, *Chin. Phys. C* **45**, 063108 (2021), arXiv:2104.00439 [hep-ph].
- [6] E. Wang, L.-S. Geng, J.-J. Wu, J.-J. Xie, and B.-S. Zou, Review of the Low-Lying Excited Baryons  $\Sigma^*(1/2^-)$ , *Chin. Phys. Lett.* **41**, 101401 (2024), arXiv:2406.07839 [hep-ph].
- [7] J.-J. Wu, R. Molina, E. Oset, and B. S. Zou, Prediction of narrow  $N^*$  and  $\Lambda^*$  resonances with hidden charm above 4 GeV, *Phys. Rev. Lett.* **105**, 232001 (2010), arXiv:1007.0573 [nucl-th].
- [8] S. Capstick and W. Roberts,  $N\pi$  decays of baryons in a relativized model, *Phys. Rev. D* **47**, 1994 (1993).
- [9] N. Isgur and G. Karl, Positive Parity Excited Baryons in a Quark Model with Hyperfine Interactions, *Phys. Rev. D* **19**, 2653 (1979), [Erratum: Phys.Rev.D 23, 817 (1981)].
- [10] M. Ablikim et al. (BESIII), Future Physics Programme of BESIII, *Chin. Phys. C* **44**, 040001 (2020), arXiv:1912.05983 [hep-ex].
- [11] S. Navas et al. (Particle Data Group), Review of particle physics, *Phys. Rev. D* **110**, 030001 (2024).
- [12] M. Ablikim et al. (BESIII), Design and Construction of the BESIII Detector, *Nucl. Instrum. Meth. A* **614**, 345 (2010), arXiv:0911.4960 [physics.ins-det].
- [13] C. Yu et al., BEPCII Performance and Beam Dynamics Studies on Luminosity, in *7th International Particle Accelerator Conference* (2016) p. TUYA01.
- [14] J. Lu, Y. Xiao, and X. Ji, Online monitoring of the center-of-mass energy from real data at BESIII, *Radiat. Detect. Technol. Methods* **4**, 337 (2020).
- [15] J.-W. Zhang et al., Suppression of top-up injection backgrounds with offline event filter in the BESIII experiment, *Radiat. Detect. Technol. Methods* **6**, 289 (2022).
- [16] X. Li et al., Study of MRPC technology for BESIII endcap-TOF upgrade, *Radiat. Detect. Technol. Methods* **1**, 13 (2017).
- [17] Y.-X. Guo et al., The study of time calibration for upgraded end cap TOF of BESIII, *Radiat. Detect. Technol. Methods* **1**, 15 (2017).
- [18] P. Cao et al., Design and construction of the new BESIII endcap Time-of-Flight system with MRPC Technology, *Nucl. Instrum. Meth. A* **953**, 163053 (2020).
- [19] S. U. Chung, Helicity coupling amplitudes in tensor formalism, *Phys. Rev. D* **48**, 1225 (1993), [Erratum: Phys.Rev.D 56, 4419 (1997)].
- [20] S. U. Chung, A General formulation of covariant helicity coupling amplitudes, *Phys. Rev. D* **57**, 431 (1998).
- [21] V. Shklyar, H. Lenske, and U. Mosel,  $\eta$ -meson production in the resonance-energy region, *Phys. Rev. C* **87**, 015201 (2013), arXiv:1206.5414 [nucl-th].
- [22] V. Sokhoyan et al. (CBELSA/TAPS), High-statistics study of the reaction  $\gamma p \rightarrow p 2\pi^0$ , *Eur. Phys. J. A* **51**, 95 (2015), [Erratum: Eur.Phys.J.A 51, 187 (2015)], arXiv:1507.02488 [nucl-ex].
- [23] B. C. Hunt and D. M. Manley, Updated determination of  $N^*$  resonance parameters using a unitary, multichannel formalism, *Phys. Rev. C* **99**, 055205 (2019), arXiv:1810.13086 [nucl-ex].
- [24] E. Golovatch et al. (CLAS), First results on nucleon resonance photocouplings from the  $\gamma p \rightarrow \pi^+\pi^-p$  reaction, *Phys. Lett. B* **788**, 371 (2019), arXiv:1806.01767 [nucl-ex].
- [25] J. Z. Bai et al. (BES), Study of  $N^*$  production from  $J/\psi \rightarrow p\bar{p}\eta$ , *Phys. Lett. B* **510**, 75 (2001), arXiv:hep-ex/0105011.
- [26] M. Ablikim et al. (BESIII), Observation of two new  $N^*$  resonances in the decay  $\psi(3686) \rightarrow p\bar{p}\pi^0$ , *Phys. Rev. Lett.* **110**, 022001 (2013), arXiv:1207.0223 [hep-ex].
- [27] M. Ablikim et al. (BESIII), Observation of a New Excited  $\Sigma$  State in  $\psi(3686) \rightarrow \bar{p}K^+\Sigma^0 + c.c.$ , (2026), arXiv:2602.11501 [hep-ex].
- [28] M. Ablikim et al. (BESIII), Partial wave analyses of  $\psi(3686) \rightarrow p\bar{p}\pi^0$  and  $\psi(3686) \rightarrow p\bar{p}\eta$ , *Phys. Rev. D* **111**, 032011 (2025), arXiv:2412.06247 [hep-ex].
- [29] M. Ablikim et al. (BESIII), Measurement of  $\psi(3686) \rightarrow \Lambda\bar{\Lambda}\eta$  and  $\psi(3686) \rightarrow \Lambda\bar{\Lambda}\pi^0$  decays, *Phys. Rev. D* **106**, 072006 (2022), arXiv:2207.14350 [hep-ex].
- [30] M. Ablikim et al. (BESIII), Study of  $\psi(3686) \rightarrow \Lambda\bar{\Lambda}\omega$ , *Phys. Rev. D* **106**, 112011 (2022), arXiv:2207.11666 [hep-ex].
- [31] M. Ablikim et al. (BESIII), Determination of Spin-Parity Quantum Numbers for the Narrow Structure near the  $p\bar{\Lambda}$  Threshold in  $e^+e^- \rightarrow pK^-\bar{\Lambda} + c.c.$ , *Phys. Rev. Lett.* **131**, 151901 (2023), arXiv:2303.01989 [hep-ex].
- [32] M. Ablikim et al. (BESIII), Precise measurement of the branching fractions of  $J/\psi \rightarrow \bar{\Lambda}\pi^+\Sigma^- + c.c.$  and  $J/\psi \rightarrow \bar{\Lambda}\pi^-\Sigma^+ + c.c.$ , *Phys. Rev. D* **108**, 112012 (2023), arXiv:2306.10319 [hep-ex].
- [33] M. Ablikim et al. (BESIII), Partial wave analysis of  $\psi(3686) \rightarrow \Lambda\bar{\Sigma}^0\pi^0 + c.c.$ , *JHEP* **02**, 212, arXiv:2408.00495 [hep-ex].
- [34] S. U. Chung, J. Brose, R. Hackmann, E. Klempt, S. Spanier, and C. Strassburger, Partial wave analysis in K matrix formalism, *Annalen Phys.* **4**, 404 (1995).
- [35] D. Jido, J. A. Oller, E. Oset, A. Ramos, and U. G. Meissner, Chiral dynamics of the two  $\Lambda(1405)$  states, *Nucl. Phys. A* **725**, 181 (2003), arXiv:nucl-th/0303062.
- [36] U. Loring, B. C. Metsch, and H. R. Petry, The Light baryon spectrum in a relativistic quark model with instanton induced quark forces: The Strange baryon spectrum, *Eur. Phys. J. A* **10**, 447 (2001), arXiv:hep-ph/0103290.
- [37] M. Ablikim et al. (BESIII), Amplitude analysis and branching fraction measurement of  $J/\psi \rightarrow \Lambda\bar{\Sigma}^0\eta + c.c.$ , (2026), arXiv:2601.07617 [hep-ex].
- [38] H. Zhang, J. Tulpan, M. Shrestha, and D. M. Manley, Multichannel parametrization of  $\bar{K}N$  scattering amplitudes and extraction of resonance parameters, *Phys. Rev. C* **88**, 035205 (2013), arXiv:1305.4575 [hep-ph].
- [39] A. V. Sarantsev, M. Matveev, V. A. Nikonov, A. V. Anisovich, U. Thoma, and E. Klempt, Hyperon II: Properties of excited hyperons, *Eur. Phys. J. A* **55**, 180 (2019), arXiv:1907.13387 [nucl-ex].
- [40] C. Menapara and A. K. Rai, Hadron Spectroscopy: Light, Strange Baryons, *Few Body Syst.* **65**, 63 (2024), arXiv:2405.06417 [hep-ph].
- [41] M. Ablikim et al. (BESIII), Observation of the decay  $\psi(3686) \rightarrow \Sigma^0\bar{\Sigma}^0\omega$ , *10.1103/PhysRevD.111.092007* (2025), arXiv:2503.18620 [hep-ex].
- [42] M. Ablikim et al. (BESIII), Observation of  $\Lambda_c^+ \rightarrow \Lambda a_0(980)^+$  and Evidence for  $\Sigma(1380)^+$  in  $\Lambda_c^+ \rightarrow \Lambda\pi^+\eta$ , *Phys. Rev. Lett.* **134**, 021901 (2025), arXiv:2407.12270 [hep-ex].
- [43] J.-J. Wu, S. Dulat, and B. S. Zou, Evidence for a new  $\Sigma^*$  resonance with  $J^P = 1/2^-$  in the old data of  $K^-p \rightarrow \Lambda\pi^+\pi^-$  reaction, *Phys. Rev. D* **80**, 017503 (2009), arXiv:0906.3950 [hep-ph].
- [44] J.-J. Xie and L.-S. Geng,  $\Sigma_{1/2^-}^*(1380)$  in the  $\Lambda_c^+ \rightarrow \eta\pi^+\Lambda$  decay, *Phys. Rev. D* **95**, 074024 (2017), arXiv:1703.09502 [hep-ph].
- [45] R. T. Ross, T. Buran, J. L. Lloyd, J. H. Mulvey, and D. Radojicic,  $\Xi\pi$  resonance with mass 1606 MeV/c<sup>2</sup>, *Phys. Lett. B* **38**, 177 (1972).
- [46] A. d. Bellefon, A. Berthon, and P. Billoir, Reactions  $K^-p \rightarrow \Xi^-K^+\pi^0$  between 2210 and 2435 MeV Ecm, *Nuovo Cim. A*

- 28**, 289 (1975).
- [47] E. Briefel *et al.*, Search for  $\Xi^*$  Production in  $K^-p$  Interactions at 2.87 GeV/c, *Phys. Rev. D* **16**, 2706 (1977).
- [48] M. Sumihama *et al.* (Belle), Observation of  $\Xi(1620)^0$  and evidence for  $\Xi(1690)^0$  in  $\Xi_c^+ \rightarrow \Xi^- \pi^+ \pi^+$  decays, *Phys. Rev. Lett.* **122**, 072501 (2019), arXiv:1810.06181 [hep-ex].
- [49] M. Ablikim *et al.* (BESIII), Measurement of the cross section for  $e^+e^- \rightarrow \Xi^- \Xi^+$  and observation of an excited  $\Xi$  baryon, *Phys. Rev. Lett.* **124**, 032002 (2020), arXiv:1910.04921 [hep-ex].
- [50] M. I. Adamovich *et al.* (WA89), Production of  $\Xi^*$  resonances in  $\Sigma^-$  induced reactions at 345 GeV/c, *Eur. Phys. J. C* **11**, 271 (1999), arXiv:hep-ex/9907021.
- [51] M. Ablikim *et al.* (BESIII), Study of excited  $\Xi$  states in  $\psi(3686) \rightarrow \bar{K}^- \Lambda \Xi^+ + \text{c.c.}$ , *Phys. Rev. D* **109**, 072008 (2024), arXiv:2308.15206 [hep-ex].
- [52] R. Molina, W.-H. Liang, C.-W. Xiao, Z.-F. Sun, and E. Oset, Two states for the  $\Xi(1820)$  resonance, *Phys. Lett. B* **856**, 138872 (2024), arXiv:2309.03618 [hep-ph].
- [53] J. Yelton *et al.* (Belle), Observation of an Excited  $\Omega^-$  Baryon, *Phys. Rev. Lett.* **121**, 052003 (2018), arXiv:1805.09384 [hep-ex].
- [54] S. Jia *et al.* (Belle), Observation of  $\Omega(2012)^- \rightarrow \Xi(1530)\bar{K}$  and measurement of the effective couplings of  $\Omega(2012)^-$  to  $\Xi(1530)\bar{K}$  and  $\Xi\bar{K}$ , *Phys. Lett. B* **860**, 139224 (2025), arXiv:2207.03090 [hep-ex].
- [55] S. Capstick and N. Isgur, Baryons in a relativized quark model with chromodynamics, *Phys. Rev. D* **34**, 2809 (1986).
- [56] R. N. Faustov and V. O. Galkin, Strange baryon spectroscopy in the relativistic quark model, *Phys. Rev. D* **92**, 054005 (2015), arXiv:1507.04530 [hep-ph].
- [57] M. Pervin and W. Roberts, Strangeness -2 and -3 baryons in a constituent quark model, *Phys. Rev. C* **77**, 025202 (2008), arXiv:0709.4000 [nucl-th].
- [58] Y. Oh,  $\Xi$  and  $\Omega$  baryons in the Skyrme model, *Phys. Rev. D* **75**, 074002 (2007), arXiv:hep-ph/0702126.
- [59] G. P. Engel, C. B. Lang, D. Mohler, and A. Schäfer (BGR), QCD with Two Light Dynamical Chirally Improved Quarks: Baryons, *Phys. Rev. D* **87**, 074504 (2013), arXiv:1301.4318 [hep-lat].
- [60] K.-L. Wang, J. Wang, Y.-K. Hsiao, and X.-H. Zhong, Excited  $\Omega$  hyperon in charmful  $\Omega_b$  weak decays, *Phys. Rev. D* **111**, 114028 (2025), arXiv:2412.02464 [hep-ph].
- [61] Q.-H. Shen, J.-X. Lu, L.-S. Geng, X. Liu, and J.-J. Xie, Radiative decays of the  $\Omega(2012)$  as a hadronic molecule, *Phys. Rev. D* **113**, 036014 (2026), arXiv:2510.13623 [hep-ph].
- [62] M. Ablikim *et al.* (BESIII), Evidence for Two Excited  $\Omega^-$  Hyperons, *Phys. Rev. Lett.* **134**, 131903 (2025), arXiv:2411.11648 [hep-ex].
- [63] R. G. Edwards, N. Mathur, D. G. Richards, and S. J. Wallace (Hadron Spectrum), Flavor structure of the excited baryon spectra from lattice QCD, *Phys. Rev. D* **87**, 054506 (2013), arXiv:1212.5236 [hep-ph].
- [64] S.-Q. Luo and X. Liu, Identifying triple-strangeness  $\Omega$  hyperons in light of recent experimental results, *Phys. Rev. D* **112**, 014047 (2025), arXiv:2504.14648 [hep-ph].
- [65] F.-C. Han, Z.-W. Liu, D. B. Leinweber, and A. W. Thomas, Structure of the  $\Omega^-(2012)$  with Hamiltonian effective field theory, *Phys. Rev. D* **112**, L051503 (2025), arXiv:2507.06682 [hep-ph].
- [66] E. B. Levicev, A. N. Skrinsky, G. M. Tumaikin, and Y. M. Shatunov, Electron-positron beam collision studies at the Budker Institute of Nuclear Physics, *Phys. Usp.* **61**, 405 (2018).
- [67] M. Achasov *et al.*, STCF conceptual design report (Volume 1): Physics & detector, *Front. Phys. (Beijing)* **19**, 14701 (2024), arXiv:2303.15790 [hep-ex].